Biogeosciences

Seasonal variability of tropical wetland CH_4 emissions: the role of the methanogen-available carbon pool

A. A. Bloom, P. I. Palmer, A. Fraser, and D. S. Reay

School of GeoSciences, University of Edinburgh, Edinburgh, UK

Correspondence to: A. A. Bloom (a.bloom@ed.ac.uk)

Abstract. We develop a dynamic methanogen-available carbon model (DMCM) to quantify the role of the methanogen-available carbon pool in determining the spatial and temporal variability of tropical wetland CH_4 emissions over seasonal timescales. We fit DMCM parameters to satellite observations of CH_4 columns from SCIAMACHY CH_4 and equivalent water height (EWH) from GRACE. Over the Amazon River basin we found substantial seasonal variability of this carbon pool (coefficient of variation $= 28 \pm 22$ %) and a rapid decay constant ($\phi = 0.017$ day^{-1}), in agreement with available laboratory measurements, suggesting that plant litter is likely the prominent methanogen carbon source over this region. Using the DMCM we derived global CH_4 emissions for 2003–2009, and determined the resulting seasonal variability of atmospheric CH_4 on a global scale using the GEOS-Chem atmospheric chemistry and transport model. First, we estimated that tropical emissions amounted to 111.1 Tg CH_4 yr^{-1}, of which 24 % was emitted from Amazon wetlands. We estimated that annual tropical wetland emissions increased by 3.4 Tg CH_4 yr^{-1} between 2003 and 2009. Second, we found that the model was able to reproduce the observed seasonal lag of CH_4 concentrations peaking 1–3 months before peak EWH values. We also found that our estimates of CH_4 emissions substantially improved the comparison between the model and observed CH_4 surface concentrations ($r = 0.9$). We anticipate that these new insights from the DMCM represent a fundamental step in parameterising tropical wetland CH_4 emissions and quantifying the seasonal variability and future trends of tropical CH_4 emissions.

1 Introduction

Wetlands are the single largest source of methane (CH_4) into the atmosphere and account for 20–40 % of the global CH_4 source (Denman et al., 2007; Ito and Inatomi, 2012), of which tropical wetlands account for 50–60 % of this global wetland CH_4 source (e.g. Cao et al., 1996; Bloom et al., 2010). Tropical wetland biogeochemistry is poorly understood compared to boreal peatlands (Mitsch et al., 2010), resulting in large inter-model discrepancies of the magnitude and distribution of tropical wetland CH_4 emission estimates (Riley et al., 2011). Tropical climate variability (e.g. resulting in widespread droughts, Lewis et al., 2011) can lead to large year to year variations in tropical wetland CH_4 emissions and subsequently the global CH_4 budget (Hodson et al., 2011). Moreover, Bousquet et al. (2011) found substantial disagreements between tropical wetland CH_4 emissions from process-based and atmospheric inversion estimates. An improved quantitative understanding of the magnitude, distribution, and variation of tropical wetland CH_4 emissions is therefore essential to further understanding of the global CH_4 cycle. Here, we parameterise tropical wetland CH_4 emissions, and hence introduce a predictive capability that can be used to determine future emissions and to help quantify global CH_4 climate feedbacks.

In wetlands and rice paddies, methanogenesis (the biogenic production of CH_4) occurs as the final step of anoxic organic matter decomposition (Neue et al., 1997). Factors influencing methanogenesis rates include substrate availability, soil pH, temperature, water table position and redox potential (Whalen, 2005). Wetland vegetation type and aquatic herbivore activity can also affect the transport of CH_4 between the soil and atmosphere (Joabsson et al., 1999; Dingemans et al.,

2011). On a global scale, seasonal variations in wetland CH$_4$ fluxes are mostly determined by temporal changes in wetland water volume and soil temperature (Walter et al., 2001; Gedney et al., 2004), and from seasonal changes in wetland extent and wetland water table depth (Ringeval et al., 2010; Bloom et al., 2010). Recent work that used SCIAMACHY lower tropospheric CH$_4$ column concentrations and Gravity Recovery And Climate Experiment (GRACE) equivalent water height (EWH) retrievals showed that the seasonality of wetland CH$_4$ emissions can be largely explained by seasonal changes in surface temperature and water volume (Bloom et al., 2010). The Amazon and Congo River basins were the only major exceptions in this study, where CH$_4$ concentrations peaked several weeks before EWH, highlighting our incomplete understanding of the processes controlling tropical wetland CH$_4$ emissions over seasonal timescales.

In this paper we focus on the seasonal lag between CH$_4$ emissions and flooding over the Amazon River basin area (Oki and Sud, 1998). We use SCIAMACHY CH$_4$ retrievals and GRACE EWH (both described in Sect. 2.2) to determine the seasonal lag between wetland CH$_4$ emissions and wetland water volume. Figure 1 shows that seasonal flooding of the Amazon basin occurs typically 1–3 months after the peak CH$_4$ concentrations, and to a lesser extent the lag persists throughout tropical wetland areas. Although typical time-lags between EWH and CH$_4$ in the Congo River basin are comparable (0–2 months), in this paper we choose to focus on the Amazon basin as it covers a larger areal extent, and larger time-lags between EWH and CH$_4$ are found over this river basin. In Sect. 2, we test the hypothesis that this lag is related to the depletion of methanogen-available carbon during the onset of the tropical wet season by explicitly accounting for this carbon pool in a parameterised model of tropical wetland CH$_4$ emissions (Bloom et al., 2010). We optimise model parameters by fitting them to SCIAMACHY CH$_4$ column and GRACE EWH measurements, and use the resulting model to estimate global wetland emission estimates. In Sect. 3 we (1) compare our results to previous estimates of wetland CH$_4$ emissions and to decomposition rates of methanogen-available carbon in anaerobic environments; (2) provide an overview of additional factors which potentially influence the seasonal variability of CH$_4$ emissions in tropical wetlands; and (3) use our estimated emissions to drive the GEOS-Chem atmospheric chemistry model as an approach to test the consistency between our emission estimates and observed variations of atmospheric CH$_4$ concentration. We conclude the paper in Sect. 4.

2   Process-based model and application

Here, we introduce a methanogen-available carbon pool (C_μ) that typically originates from labile plant litter, recalcitrant organic matter decomposition and root exudates (e.g. Wania et al., 2010). Typically, soil carbon pool decay

constants are more than an order of magnitude lower than those of leaf litter (Sitch et al., 2003; Wania et al., 2010). Therefore, if C_μ originates mostly from the slow-decomposing recalcitrant carbon pool, then variations in C_μ over seasonal timescales are likely to be small. Conversely, if C_μ is drawn from leaf litter, then large variations in C_μ abundance may arise as a result of rapid litter decomposition in the tropics. Miyajima et al. (1997) measured CH$_4$ accumulation of anaerobic decomposition of incubated tropical withered tree leaves over a 200 day period. These observations showed a rapid decrease in decomposition rates over the incubation period. Bianchini Jr. et al. (2010) found similar results for anaerobic decomposition from dried and ground *Oxycaryum cubense* at 20 °C: following a 20-day lag (where no emissions were observed) CH$_4$ produced from organic carbon decomposition peaked after a 50-day period, and then rapidly decreased. On a tropical river-basin scale, flooded areas expand at the onset of the wet season and engulf newly available plant litter; as a result, CH$_4$ emissions from plant litter may peak before the height of the water table. The occurrence of anaerobic CH$_4$ emissions from litter decomposition within sub-seasonal timescales raises the question as to whether C_μ significantly varies in time.

2.1   Model description

We base our model on previous work (Bloom et al., 2010) that describes the temporal variability of wetland emissions $F_{\text{CH}_4}^t$ (mg CH$_4$ m^{-2} day^{-1}) as a function of EWH and surface temperature:

$$F_{\text{CH}_4}^t = k(\Gamma_{\text{w}}^t + D_\alpha) Q_{10}(T_{\text{s}})^{\frac{T_{\text{s}}^t}{10}}, \tag{1}$$

where at time t (days), Γ_{w}^t is the EWH, T_{s}^t is the surface temperature (K), D_α is the equivalent depth of the wetland soil (m), $Q_{10}(T_{\text{s}})$ is the temperature dependence function implemented by Gedney et al. (2004), and k is a scaling constant (mg CH$_4$ m^{-2} day^{-1}) accounting for all temporally constant factors (e.g. Gedney et al., 2004).

Equation (1) assumes an inexhaustible source of methanogen-available carbon. Here, we account for the potential seasonal changes in C_μ by substituting k with $\phi_0 C_\mu^t$, where ϕ_0 (day^{-1}) is the temperature, water and carbon independent decay constant of wetland methanogenesis, and C_μ^t is the value of C_μ (mg CH$_4$ m^{-2}) at time t:

$$F_{\text{CH}_4}^t = \phi_0 C_\mu^t (\Gamma_{\text{w}}^t + D_\alpha) Q_{10}(T_{\text{s}})^{\frac{T_{\text{s}}^t}{10}}. \tag{2}$$

To determine temporal changes in C_μ, we define C_μ^{t+1} in terms of C_μ^t:

$$C_\mu^{t+1} = C_\mu^t + N_\mu \Delta t - F_{\text{CH}_4}^t \Delta t, \tag{3}$$

where Δt is the time interval, $F_{\text{CH}_4}^t$ is the carbon loss due to emitted CH$_4$ (Eq. 2), and N_μ is the net influx of carbon
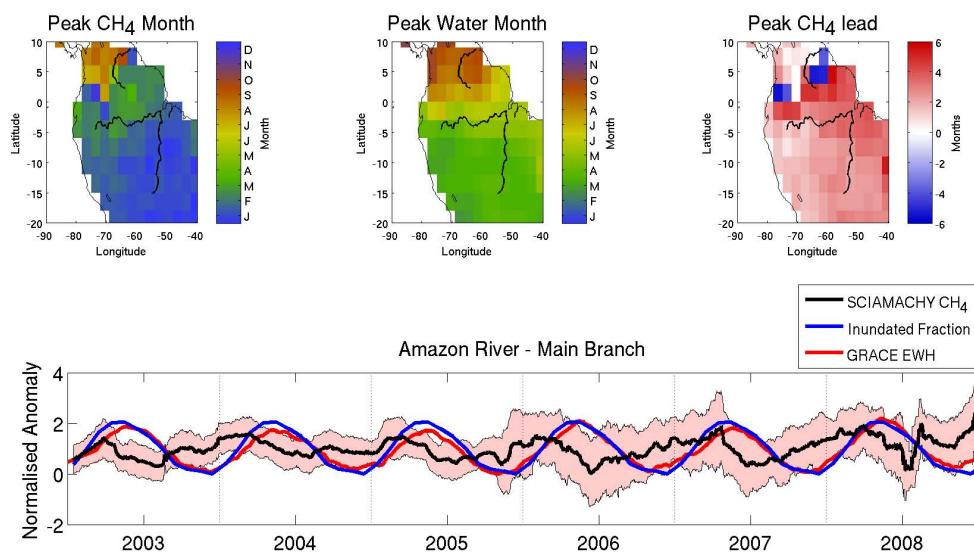
Fig. 1. Top: The timing (month of year) of peak CH$_4$ concentrations from SCIAMACHY (left), peak equivalent water height (EWH) from GRACE (middle), and the peak CH$_4$ concentration lead over tropical South America (right). Bottom: Normalised anomaly of GRACE EWH, mean flood fraction (Prigent et al., 2007), and mean CH$_4$ concentrations (including 1-standard deviation envelope) over the main branch of the Amazon River (0°–6° S, 40°–80° W).

available for methanogenesis from plant litter, root exudates, and breakdown of complex polymers from the recalcitrant carbon pool. We assume N_μ is temporally constant, and we assume wetland carbon stocks are in quasi-equilibrium on annual timescales, hence $\overline{N_\mu} = \overline{F^t_{CH_4}}$. Note that when ϕ_0 is small, the equilibrium $C_\mu \gg N_\mu \Delta t$. In this case, $C_\mu^{t+1} \simeq C_\mu^t$ and Eq. (2) converges to Eq. (1) (Bloom et al., 2010), which assumes $\phi_0 C_\mu$ is constant over seasonal timescales. In order to compare derived decay constants with observed and model values (e.g. Miyajima et al., 1997; Wania et al., 2010), we determine the annual mean decay constant of wetlands areas as $\overline{\phi} = \overline{F^t_{CH_4}}/\overline{C^t_\mu}$ (day^{-1}). Equations (2) and (3) constitute the dynamic methanogen-available carbon model (DMCM).

2.2 Data

For the sake of brevity, we only include a brief description of the datasets for our analysis and refer the reader to dedicated papers. Solar backscatter data from the Scanning Imaging Absorption Spectrometer for Atmospheric Cartography (SCIAMACHY) instrument onboard Envisat was used to retrieve the mean column concentrations of CH$_4$ in the atmosphere (Frankenberg et al., 2005). The spatial resolution of CH$_4$ retrievals is 30 km × 60 km, and the Envisat orbital geometry ensures global coverage at 6-day intervals. CH$_4$ retrievals were only achievable in daytime cloud-free conditions. The Gravity Recovery and Climate Experiment (GRACE) is a twin satellite system from which the Earth's gravity field was retrieved at 10-day intervals. Tides, atmospheric pressure and wind are included in the applied corrections on GRACE gravity retrievals; the remaining

temporal variation in GRACE gravity is dominated by terrestrial water variability (Tapley et al., 2004). We incorporated SCIAMACHY CH$_4$ concentrations, GRACE EWH and NCEP/NCAR daily 1.9° × 1.88° temperature re-analyses (Kalnay et al., 1996) into a process-based model following Bloom et al. (2010). We used the 2003–2008 SCIAMACHY column CH$_4$ retrievals (Frankenberg et al., 2008), and the CNES GRACE EWH 1° × 1° 10-day resolution product (Lemoine et al., 2007). We aggregated all three datasets to a daily 3° × 3° horizontal grid (see Bloom et al., 2010).

2.3 Global parameter optimisation

We implemented the DMCM (as shown in Eqs. (2) and (3)) on a global 3° × 3° grid for the period 2003–2009. We drove the DMCM using the aggregated daily values of T^t_s and Γ^t_w. We spun up the DMCM using 2003 T^t_s and Γ^t_w values until it reached an annual equilibrium ($\overline{N_\mu} = \overline{F^t_{CH_4}}$). In contrast to Bloom et al. (2010), we supplemented the $Q_{10}(T_s)$ function with a gradual linear cut-off for temperatures for $0\,°C < T^t_s < -10\,°C$, and when $T^t_s < -10\,°C$, $F^t_{CH_4} = 0$ as a first order approximation to wintertime CH$_4$ emission inhibition in boreal wetlands. As the Q_{10} function never reached zero, this supplementary constraint effectively suppressed wintertime CH$_4$ emissions, which is broadly consistent with our current understanding of CH$_4$ emissions in boreal wetlands.

We applied the DMCM globally in order to determine (i) the magnitude of $\overline{\phi}$ and C_μ in the tropics within each 3° × 3° gridcell, (ii) the potential of C_μ temporal variability on extratropical wetland environments, and (iii) CH$_4$ emissions from wetlands and rice paddies at a global scale. We determined

the global distribution and seasonal variability of wetland CH$_4$ emissions by optimising parameters ϕ_0 and D_α at each gridcell by minimising the following cost function (J):

$$J = \sum_{t=1}^{n}(\kappa \times \Delta F_{CH_4}^t - \Delta S_{CH_4}^t)^2, \qquad (4)$$

where $\Delta S_{CH_4}^t$ denotes the SCIAMACHY CH$_4$ variability, $\Delta F_{CH_4}^t$ is derived from Eqs. (2) and (3), and the conversion factor κ (ppm kg^{-1} CH$_4$ m^{-2} day^{-1}) relates CH$_4$ emissions to the equivalent column concentration in the lower troposphere (see Bloom et al., 2010). We removed the interannual trend (represented as a second order polynomial) from $\Delta S_{CH_4}^t$ in order to minimize the influence of global atmospheric CH$_4$ trends. We then implemented the global $Q_{10}(T_s)$ optimisation approach of Bloom et al. (2010). Like other top-down parameter optimisation methods of global wetland CH$_4$ emissions (Gedney et al., 2004; Bloom et al., 2010), our method was unable to distinguish between the seasonality of CH$_4$ emissions from wetlands and rice paddies due to the concurring fluxes over seasonal timescales. However we anticipated that varying fertilisation and irrigation practices also influence the seasonality in rice paddy CH$_4$ emissions (Conen et al., 2010). We hence distinguished the sources spatially (Bloom et al., 2010), for which we had more confidence in the distribution of rice paddies. Finally, we used the IPCC global wetland and rice paddy CH$_4$ emissions median of 227.5 Tg CH$_4$ yr^{-1} (Denman et al., 2007) as a base value for 2003 emissions.

We propagated the following uncertainties through our global wetland and rice paddy CH$_4$ emissions estimation (Bloom et al., 2010): (i) SCIAMACHY CH$_4$ observation errors; (ii) the uncertainty of the linear fit between $F_{CH_4}^t$ and $S_{CH_4}^t$; (iii) the uncertainty $\sigma_\kappa = \pm 16\%$ associated with κ; and (iv) a global wetland and rice paddy uncertainty of $\pm$ 58 Tg CH$_4$ yr^{-1} (Denman et al., 2007).

We propagated SCIAMACHY CH$_4$ VMR errors to a 3$°$ × 3$°$ resolution; compared to a global mean of $\pm$18.0 ppb, we found mean CH$_4$ error values of $\pm$19.2 ppb (5th–95th percentile = 6.3–37.8 ppb) over the Amazon River basin. Temporal CH$_4$ VMR error variability was dominated by the number of cloud-free CH$_4$ VMR observations within each 3$°$ × 3$°$ gridcell for each daily timestep. We found little seasonal variability in the three-monthly mean propagated CH$_4$ errors (18.28–20.36 ppb). As the correlation of CH$_4$ errors within each gridcell was unknown, we chose not to weight the cost function (Eq. 4) using propagated SCIAMACHY CH$_4$ errors.

We incorporated the uncertainty of κ, $\sigma_\kappa = \pm 16\%$ in our estimated CH$_4$ emissions, where σ_κ is the estimated uncertainty between surface CH$_4$ emission amplitude and CH$_4$ column VMR amplitude; this value was derived from an atmospheric chemistry transport model (GEOS-Chem) using prior emissions and SCIAMACHY averaging kernels (Bloom et al., 2010). Finally, we implemented a global

wetland and rice paddy uncertainty equivalent to the variance of IPCC wetland emission estimates ($\pm$ 58 Tg CH$_4$ yr^{-1}).

3   Results and discussion

Over the Amazon River basin, we find wetland CH$_4$ fluxes coincide with small values of C_μ, resulting in a highly variable C_μ over seasonal timescales. Assuming an annual mean inundated fraction of 3.3 % (Prigent et al., 2007), the median CH$_4$ flux over a flooded area is 1.06 Mg C ha^{-1} yr^{-1} (387 mg CH$_4$ m^{-2} day^{-1}). The median Amazon wetland $C_\mu = 0.16$ Mg C ha^{-1} yr^{-1} with a range of 0.02–7.89 Mg C ha^{-1} yr^{-1} (5th–95th percentile). The large spatial variability of C_μ is consistent with the complexity of methanogenesis rates in wetlands (Neue et al., 1997; Whalen, 2005). Large temporal changes of C_μ are observed in the Amazon River basin, where the mean C_μ coefficient of variation (c_v) is 28 $\pm$ 22 % over the period 2003–2009. When we allow C_μ to vary in extra-tropical regions, we find a median of $c_v < 0.1$ %, and as a result the relatively small C_μ variability does not influence the seasonality of CH$_4$ emissions outside the tropics. For rice paddy areas in southeast Asia we find a median of $c_v = 4.8$ %. We acknowledge that due to the varying rice cultivation practices around the world (Conen et al., 2010), the effects of rice paddy irrigation and the timing of fertilisation on C_μ cannot be captured by the DMCM approach.

To determine whether our derived values for C_μ and $\overline{\phi}$ are relevant to tropical ecosystems, we compared them against laboratory measurements of anaerobic decomposition of withered leaves from a wetland region in Narathiwat, Thailand (Miyajima et al., 1997). We simulated CH$_4$ production from C_μ at each model gridcell for a 200-day period without fresh carbon input (N_μ=0), and we used innunded fraction observations (Prigent et al., 2007) to determine the flux magnitude over flooded areas only. Figure 2 shows the cumulative CH$_4$ production over a 200-day period for (i) simulated decomposition from derived $\overline{\phi}$ and C_μ values over the Amazon, (ii) simulated decomposition from derived $\overline{\phi}$ and C_μ values over boreal wetlands, and (iii) upscaled withered leaf mineralisation rates by Miyajima et al. (1997) using a median of 17.5 Mg C ha^{-1} yr^{-1} fine and coarse woody debris (Malhi et al., 2009). For boreal and tropical C_μ decomposition, the median cumulative CH$_4$ emissions, 68 % confidence interval, and mean decay constants ($\overline{\phi}$) are shown. For the withered leaf mineralisation rates, we show the mean fitted decay constant ($\overline{\phi}$) and the range and median cumulative CH$_4$ emissions.

The top-down parameter estimation of $\overline{\phi}$ and C_μ suggest plant litter C_μ is a fundamental component of tropical CH$_4$ emission seasonality. Our top-down estimation of anaerobic decomposition rates for tropical wetland CH$_4$ emissions compare favourably with laboratory measurements of anaerobically produced CH$_4$; while the magnitude of tropical

Table 1. Model and observed decay constants for organic matter decomposition in anaerobic environments.

	Decay Constant (yr^{-1})	Study
Amazon Wetlands ($\overline{\phi}_{\text{Amazon}}$)	2.6−9.6[a] (median=5.9)	*This Study*: Top-down wetland CH$_4$ emission parameter optimisation
Withered Leaves (35 °C)	4.0	*Miyajima et al. (1997)*: Decay constant from anaerobic tropical leaf CH$_4$ mineralisation
Wetland Macrophyte Decomposition	1.0−5.5	*Longhi et al. (2008)*[b]: Measured decomposition rates in Paluda di Ostiglia, Italy
Soil Carbon Pool (10 °C) Leaf Litter (10 °C) Root Exudates (10 °C)	0.001−0.03 0.35 13	*Wania et al. (2010)*: Bottom-up CH$_4$ Emissions from Northern Peatlands

[a] 68 % confidence interval
[b] Mass-loss decomposition rates
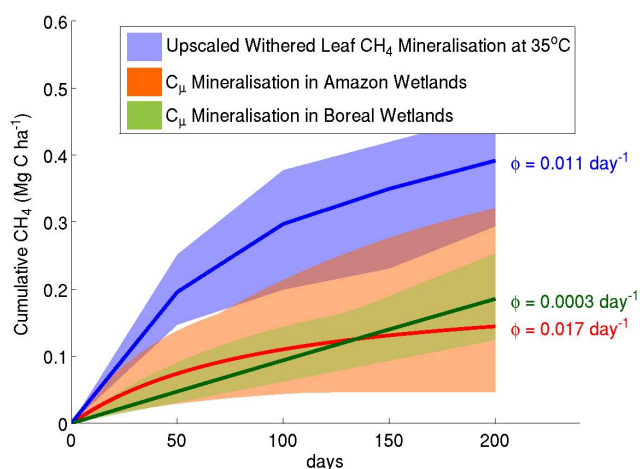
Fig. 2. Cumulative CH4 emissions over a 200-day period from model C$_\mu$ mineralisation and incubated withered leaves. Blue: median and range of values from Miyajima et al. (1997). Red (green): median and 68 % confidence interval range of CH$_4$ emissions from the Amazon River basin (boreal wetland) from C_μ and $\overline{\phi}$ values when $N_\mu = 0$. A total litter stock of 17.5 Mg C ha^{-1} (Malhi et al., 2009) was used to upscale the Miyajima et al. (1997) CH$_4$ mineralisation rates.

C_μ decomposition is more than a factor of two smaller than laboratory measurements (Miyajima et al., 1997), the mean decay constant $\overline{\phi}_{\text{Amazon}} = 0.017 \text{ day}^{-1}$ compares well to $\overline{\phi}_{\text{leaf}} = 0.011 \text{ day}^{-1}$ for withered leaf decomposition. The larger laboratory measurements (Miyajima et al., 1997) are partially explained by an incubation temperature of 35 °C (cf. a mean surface temperature in the Amazon basin of 23 °C), and the lack of observations for coarse woody debris decomposition. As a result of relatively high $\overline{\phi}$ values, measured leaf decomposition and model CH$_4$ emissions both show a significant reduction of CH$_4$ emission
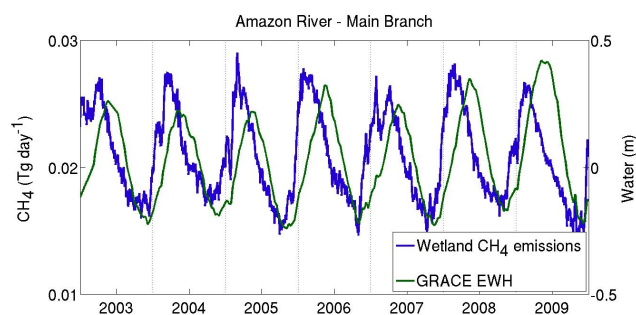
Fig. 3. Daily wetland CH$_4$ emissions for 2003–2009 (blue) and GRACE equivalent water height (green) over the central branch of the Amazon River (0°–6° S, 40°–80° W).

rates throughout the 200-day period. In contrast, the boreal decay constant ($\overline{\phi}_{\text{Boreal}} = 0.0003 \text{ day}^{-1}$) indicates relatively constant CH$_4$ emission rates throughout the 200-day period.

Table 1 shows a comparison between observed and model decay constants derived from a variety of methods. The range of $\overline{\phi}_{\text{Amazon}}$ values are within the order of magnitude of leaf and wetland macrophyte decay constants (Miyajima et al., 1997; Longhi et al., 2008; Wania et al., 2010). We believe that $\overline{\phi}_{\text{Amazon}}$ is an indicator for the cumulative decay constant of the rapid anaerobic decomposition of root exudates, plant litter decomposition, and the contribution of recalcitrant carbon pools. For a more detailed $\overline{\phi}_{\text{Amazon}}$ comparison with observed and model decay constant values, an estimation of the overall $\overline{\phi}$ in wetland CH$_4$ production from bottom-up process-based models (e.g. Wania et al., 2010) is needed.

Figure 3 shows the total CH$_4$ flux over the central branch of the Amazon River (0° N–6° S, 80° W–40° W). The temporal changes in C_μ result in a significantly different timing for CH$_4$ emissions over the tropics in comparison to the Bloom et al. (2010) water volume and temperature dependence
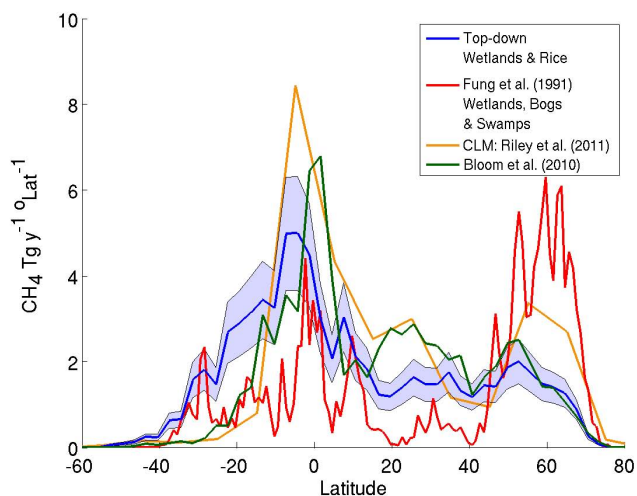
Fig. 4. Zonal profile of CH$_4$ emissions from wetlands and rice paddies: top-down wetlands and rice, this study (blue); wetlands, bogs and swamps, (Fung et al., 1991, red); wetland and rice paddy emissions (Riley et al., 2011, orange); wetland and rice paddy CH$_4$ emissions (Bloom et al., 2010, green). Riley et al. (2011) attribute their elevated tropical fluxes to anomalously high predicted net primary productivity in the Community Land Model (CLM version 4).

approach. While in the dry season the minimum CH$_4$ fluxes coincide with the lowest GRACE EWH, peak CH$_4$ fluxes occur during the rising water phase. The DMCM optimisation predicts that the accumulation of carbon in the dry season results in higher C_μ values at the onset of the wet season. This carbon pool is then rapidly depleted during the wet season. As a result, CH$_4$ emission rates begin to decrease before the peak water phase in the wet season.

In order to determine the importance of temperature variablity in estimating $\overline{\phi}$ and the C_μ coefficient of variation, c_v, we performed a temperature-driven sensitivity analysis on the DMCM. Using a range of Q$_{10}$(T_s) = 1.2 – 4 to repeat the global parameter optimisation (Sect. 2.3), we derived a corresponding ranges of $\overline{\phi}$= 0.018−0.012 and c_v = 20.2−31.3 %, respectively, for the Amazon River basin. Hence, larger C_μ seasonality is associated with higher Q$_{10}$(T_s). We note that the seasonal variability of C_μ and the relatively high turnover rates are a prominent feature in the Amazon River basin across a range of prescribed Q$_{10}$(T_s) values.

Other hypotheses that could explain the lag between CH$_4$ and EWH include the temporal variability of (a) macrophyte biomass, (b) water column oxidation, (c) redox potential, and (d) soil pH. The presence of aquatic macrophytes plays an important role in the production of methane in wetland soils, as macrophytes produce carbon available for methanogenesis, facilitate the transport of CH$_4$ to the atmosphere, transport O$_2$ to the subsurface (e.g. Laanbroek, 2010), and can inhibit light and re-aeration in aquatic envionments (Pierobon et al., 2010). Hence, an increase in macrophyte biomass during the rising water phase (e.g. Silva et al., 2009) could result

in seasonal changes in CH$_4$ emissions in tropical wetland environments due to enhanced plant-mediated transport and an increase in labile carbon in aquatic environments. Conversely, seasonal macrophyte growth may result in increased methanotrophy due to increased O$_2$ transport to the subsurface. Seasonal variability in redox potential in wetland environments is controlled by microbial activity, and hence is indirectly controlled by temperature, nutrient availability, water table level and root biomass, amongst other factors (Seybold et al., 2002; Thompson et al., 2009; Schmidt et al., 2011). However, few long-term measurements of redox potential have been performed over seasonal timescales, and further research is required to determine the large-scale redox variability in wetland environments. CH$_4$ oxidation within the water column (e.g. Schubert et al., 2010) has also been proposed as a mechanism explaining reduced CH$_4$ emissions during the peak of the wet season (Mitsch et al., 2010), although this would result in a second CH$_4$ peak at the end of the wet season. The absence of this peak in our analysis suggests this process plays only a minor role in the seasonality of tropical wetland CH$_4$ emissions. Soil pH has been found to temporally vary over seasonal timescales and, in particular, has been found to increase with decreasing redox potential (e.g. Singh, 2001; Seybold et al., 2002), although pH responses to redox potential and water table can vary widely (e.g. Singh et al., 2000; Thompson et al., 2009). Although seasonal variation in wetland pH as a significant control on CH$_4$ emissions is a viable hypothesis, to our knowledge there are currently no repeat measurements of pH in response to flooding in tropical wetlands. Other mechanisms that could temporally affect CH$_4$ emissions include the subsurface sulfur and iron cycles (Laanbroek, 2010).

We also expect uncertainties in the seasonal variability of tropical wetland CH$_4$ fluxes to arise from (i) the use of GRACE EWH as a proxy for wetland water volume and (ii) the first order approximation of a temporally constant N_μ. GRACE monthly EWH change uncertainties of 1.0–2.1 cm were reported by Wahr et al. (2004); over the Amazon River basin, EWH variability is between 0.30–0.42 m for 2003–2009. However, GRACE EWH is only a proxy for wetland water volume. Papa et al. (2008) found a strong concurrence in the seasonal cycle of GRACE EWH, inundated fraction, and modelled water storage. We also find strong seasonal covariance over the main branch of the Amazon River (Fig. 1). Although independently GRACE and inundated fraction (Prigent et al., 2007) provide proxies for wetland water volume, a better understanding of basin-scale hydrology could ultimately be achieved via a sythesis of all available hydrological parameters (e.g. Azarderakhsh et al., 2011).

We chose a constant value of $\overline{N_\mu} = \overline{F_{CH_4}}$ as a first order approximation of methanogen-available carbon input in wetlands. However, the likely factors influencing the temporal variability of N_μ are the seasonal variability of root exudates and leaf litter. While root exudates are strongly dependent on
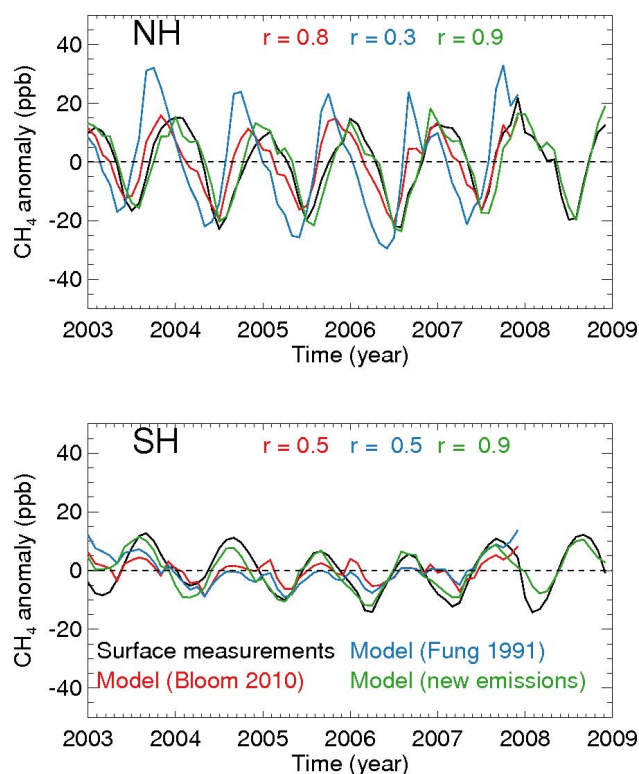
Fig. 5. Northern Hemisphere (NH, top) and Southern Hemisphere (SH, bottom) mean observed and model methane anomalies from surface concentration measurements, 2003–2008. Surface concentration measurements (black) are from the GasLab, AGAGE and ESRL networks (Francey et al., 1996; Prinn et al., 2000; Cunnold et al., 2002; Dlugokencky et al., 2009). The GEOS-Chem global 3-D chemistry transport model (Fraser et al., 2011) is driven by wetland CH$_4$ emission estimates from Fung et al. (1991) (blue), Bloom et al. (2010) (red), and our new top-down approach (green).

Table 2. Estimates of total annual Amazon River basin wetland CH$_4$ emissions (Tg CH$_4$ yr^{-1}).

Study	Amazon Wetland CH$_4$ Emissions (Tg CH$_4$ yr^{-1})
Melack et al. (2004)	22
Fung et al. (1991)	5.3
Riley et al. (2011)	58.9*
Bloom et al. (2010)	20.0
This study	26.2 ± 9.8

* High tropical fluxes by Riley et al. (2011) are a result of anomalously high predicted net primary productivity in the Community Land Model (CLM version 4).

reduction in boreal wetland emissions (3.2 %), primarily due to the introduction of a gradual cut-off in methanogenesis rates under 0 °C (Sect. 2.3). During 2003–2008, the global change in CH$_4$ wetland emissions amounted to an increase of 7.7 Tg CH$_4$ yr^{-1}, mostly as a result of boreal wetlands (3.1 Tg CH$_4$ yr^{-1}) and tropical wetlands (3.4 Tg CH$_4$ yr^{-1}), while there was also a significant increase of 1.1 Tg CH$_4$ yr^{-1} from mid-latitude wetlands. The increase in Southern Hemisphere extra-tropical wetland emissions (0.13 Tg CH$_4$ yr^{-1}) did not significantly contribute to the CH$_4$ wetland emissions growth during 2003–2008. Boreal wetland emissions increased by 1.6 Tg CH$_4$ yr^{-1} in between 2006–2007 and decreased by 0.1 Tg CH$_4$ yr^{-1} in 2007–2008. Tropical wetland emissions increased by 1.4 Tg CH$_4$ yr^{-1} in 2006–2007 and 1.2 Tg CH$_4$ yr^{-1} in 2007–2008. Other work shows a larger interannual variability, a similar year-to-year trend for boreal wetlands, and a decrease in the atmospheric CH$_4$ inversion estimates of tropical wetland emissions for 2007–2008 (Bousquet et al., 2011).

Finally, we used our wetland and rice CH$_4$ emission estimates to drive the GEOS-Chem global 3-D atmospheric chemistry and transport model (described and evaluated by Fraser et al., 2011), allowing us to test consistency between our emissions to surface measurements of CH$_4$ concentrations. We sampled the model at the time and geographical location of the surface CH$_4$ measurements from the GasLab, AGAGE and ESRL networks (Francey et al., 1996; Prinn et al., 2000; Cunnold et al., 2002; Dlugokencky et al., 2009). Figure 5 shows model and observed CH$_4$ concentration anomalies (i.e. minus the mean trend) for the Northern and Southern Hemispheres. We chose to remove the interannual trend from all CH$_4$ concentrations to compare the seasonality of model and surface measurements of CH$_4$. We show that the DMCM approach better describes the observed seasonality in both hemispheres ($r_{NH} = 0.9$, $r_{SH} = 0.9$), and the amplitude of the Southern Hemisphere seasonality is largely improved in comparison to the GEOS-Chem runs using Fung et al. (1991) and Bloom et al. (2010) CH$_4$ emissions.

NPP, in-situ and modelled estimates of leaf litter seasonality in the Amazon River basin have been found to vary widely (Chave et al., 2010; Caldararu et al., 2012). Ultimately, a temporally variable and complete representation of N_μ is required in order to further understand the temporal variability of C_μ in wetlands.

By globally integrating the DMCM method, we estimated tropical wetlands emit 111.1 Tg CH$_4$ yr^{-1}, where Amazon wetlands account for 26.2 Tg CH$_4$ yr^{-1} (24 %). Table 2 shows our estimates are within the range of other independent Amazon wetland emission CH$_4$ estimates. Figure 4 shows the zonal profile of our top-down approach with the associated uncertainty estimates. We capture three main features of global wetland and rice paddy emissions – i.e. peaks over the tropics, subtropics and lower mid-latitudes (mainly due to rice), and boreal latitudes – in agreement with previous studies (Bloom et al., 2010; Fung et al., 1991; Riley et al., 2011). In comparison to our previous work (Bloom et al., 2010), we find a slight

4 Concluding remarks

Understanding the temporal controls of temperature, water volume and carbon content of wetlands is crucial in determining the global and regional seasonal cycle of wetland CH₄ emissions. We showed that incorporating a temporally variable methanogen-available carbon pool, C_μ, in our top-down approach results in a significant improvement in describing the temporal behaviour of tropical and global CH₄ emissions.

By implementing our dynamic methanogen-available carbon model (DMCM) on a global scale, we determined the effects of a seasonally variable C_μ on the seasonality of wetland CH₄ emissions in the Amazon River basin. We found a median decay constant of $\overline{\phi}_{\text{Amazon}} = 0.017\,\text{day}^{-1}$ over the Amazon River basin. Seasonal changes in C_μ in the tropics largely explained the seasonal lag between SCIAMACHY observed CH₄ concentrations and GRACE equivalent water height. The relatively high seasonal variability in C_μ (mean $c_v = 28\,\%$) over the Amazon River basin resulted in peak CH₄ emissions occurring mostly 1–3 months prior to the peak water height period; in contrast, the median boreal C_μ variability was $c_v < 0.1\,\%$. We showed a substantial improvement in simulating the seasonality of surface concentrations when using the GEOS-Chem atmospheric chemistry transport model with our wetland and rice CH₄ emission estimates ($r = 0.9$). These improvements in the magnitude and temporal dynamics of tropical CH₄ emissions will ultimately help constrain global inverse modelling efforts.

We anticipate that this work will lead to further and more detailed parameterisation of tropical wetland CH₄ emissions, and we expect our tropical wetland CH₄ emission parameterisation will reduce the uncertainty in forecasting future changes in wetland CH₄ emissions.

References

Azarderakhsh, M., Rossow, W. B., Papa, F., Norouzi, H., and Khanbilvardi, R.: Diagnosing water variations within the Amazon basin using satellite data, J. Geophys. Res. Atmos., 116, D24107, doi:10.1029/2011JD015997, 2011.

Bianchini Jr., I., da Cunha-Santino, M. B., Romeiro, F., and Bitar, A. L.: Emissions of methane and carbon dioxide during anaerobic decomposition of aquatic macrophytes from a tropical lagoon (São Paulo, Brazil), Acta Limnologica Brasiliensia (Online), 22, 157–164, 2010.

Bloom, A. A., Palmer, P. I., Fraser, A., Reay, D. S., and Frankenberg, C.: Large-Scale Controls of Methanogenesis Inferred from Methane and Gravity Spaceborne Data, Science, 327, 322–325, 2010.

Bousquet, P., Ringeval, B., Pison, I., Dlugokencky, E. J., Brunke, E.-G., Carouge, C., Chevallier, F., Fortems-Cheiney, A., Frankenberg, C., Hauglustaine, D. A., Krummel, P. B., Langenfelds, R. L., Ramonet, M., Schmidt, M., Steele, L. P., Szopa, S., Yver, C., Viovy, N., and Ciais, P.: Source attribution of the changes in atmospheric methane for 2006–2008, Atmos. Chem. Phys., 11, 3689–3700, doi:10.5194/acp-11-3689-2011, 2011.

Caldararu, S., Palmer, P. I., and Purves, D. W.: Inferring Amazon leaf demography from satellite observations of leaf area index, Biogeosciences, 9, 1389–1404, doi:10.5194/bg-9-1389-2012, 2012.

Cao, M., Marshall, S., and Gregso, K.: Global carbon exchange and methane emissions from natural wetlands: Application of a process-based model, J. Geophys. Res., 101, 14399–14414, 1996.

Chave, J., Navarrete, D., Almeida, S., Álvarez, E., Aragão, L. E. O. C., Bonal, D., Châtelet, P., Silva-Espejo, J. E., Goret, J.-Y., von Hildebrand, P., Jiménez, E., Patiño, S., Peñuela, M. C., Phillips, O. L., Stevenson, P., and Malhi, Y.: Regional and seasonal patterns of litterfall in tropical South America, Biogeosciences, 7, 43–55, doi:10.5194/bg-7-43-2010, 2010.

Conen, F., Smith, K. A., and Yagi, K.: Methane and Climate Change, chap. Rice Cultivation, 115–135, EarthScan, ISBN 9781844078233, 2010.

Cunnold, D. M., Steele, L. P., Fraser, P. J., Simmonds, P. G., Prinn, R. G., Weiss, R. F., Porter, L. W., O'Doherty, S., Langenfelds, R. L., Krummel, P. B., Wang, H. J., Emmons, L., Tie, X. X., and Dlugokencky, E. J.: In situ measurements of atmospheric methane at GAGE/AGAGE sites during 1985–2000 and resulting source inferences, J. Geophys. Res. Atmos., 107, 4225, doi:10.1029/2001JD001226, 2002.

Denman, K., Brasseur, G., Chidthaisong, A., Ciai, P., Cox, P., Dickinson, R., Hauglustaine, D., Heinze, C., Holland, E., Jacob, D., U.Lohmann, Ramachandran, S., da Silva Dias, P., Wofsy, S., and Zhang, X.: Couplings Between Changes in the Climate System and Biogeochemistry, in: Climate Change 2007: The Physical Science Basis. Contribution of Working Group I to the Fourth Assessment Report of the Intergovernmental Panel on Climate Change, edited by: Solomon, S., Qin, D., Manning, M., Chen, Z., Marquis, M., Averyt, K. B., Tignor, M., and Miller, H. L., Cambridge University Press, Cambridge, UK and New York, NY, USA, 2007.

Dingemans, B., Bakker, E., and Bodelier, P.: Aquatic herbivores facilitate the emission of methane from wetlands, Ecology, 92, 1166–1173, 2011.

Dlugokencky, E. J., Lang, P., and Masarie, K.: Atmospheric Methane Dry Air Mole Fractions from the NOAA ESRL Carbon Cycle Cooperative Global Air Sampling Network, 1983–2007, Version: 2008-07-02, 2009.

Francey, R. L., Steele, L., Langenfelds, R., Lucarelli, M., Allison, C., Beardsmore, D., Coram, S., Derek, N., de Silva, F., Etheridge, D., Fraser, P., Henry, R., Turner, B., Welch, E., Spencer, D., and Cooper, L.: Global Atmospheric Sampling Laboratory (GASLAB): supporting and extending the Cape Grim trace gas programs. Baseline Atmospheric Program (Australia) 1993, edited by: Francey, R. J., Dick, A. L., and Derek, N., 8–29, Bureau of Meteorology and CSIRO Division of Atmospheric Research, Melbourne, Australia, 1996.

Frankenberg, C., Meirink, J. F., van Weele, M., Platt, U., and Wagner, T.: Assessing Methane Emissions from Global Space-Borne Observations, Science, 308, 1010–1014, 2005.

Frankenberg, C., Warneke, T., Butz, A., Aben, I., Hase, F., Spietz, P., and Brown, L. R.: Pressure broadening in the $2\nu_3$ band of methane and its implication on atmospheric retrievals, Atmos. Chem. Phys., 8, 5061–5075, doi:10.5194/acp-8-5061-2008, 2008.

Fraser, A., Miller, C. C., Palmer, P. I., Deutscher, N. M., Jones, N. B., and Griffith, D. W. T.: The Australian methane budget: Interpreting surface and train-borne measurements using a chemistry transport model, J. Geophys. Res., 116, D20306, doi:10.1029/2011JD015964, 2011.

Fung, I., John, J., Lerner, J., Matthews, E., Prather, M., Steele, L. P., and Fraser, P. J.: Three-dimensional model synthesis of the global methane cycle, J. Geophys. Res., 96, 13033–13065, doi:10.1029/91JD01247, 1991.

Gedney, N., Cox, P. M., and Huntingford, C.: Climate feedback from wetland methane emissions, Geophys. Res. Lett., 31, L20503, doi:10.1029/2004GL020919, 2004.

Hodson, E. L., Poulter, B., Zimmermann, N. E., Prigent, C., and Kaplan, J. O.: The El Niño-Southern Oscillation and wetland methane interannual variability, Geophys. Res. Lett., 38, L08810, doi:10.1029/2011GL046861, 2011.

Ito, A. and Inatomi, M.: Use of a process-based model for assessing the methane budgets of global terrestrial ecosystems and evaluation of uncertainty, Biogeosciences, 9, 759–773, doi:10.5194/bg-9-759-2012, 2012.

Joabsson, A., Christensen, T. R., and Wallen, B.: Vascular plant controls on methane emissions from northern peatforming wetlands, Trends in Ecology and Evolution, 14, 385–388, 1999.

Kalnay, E., Kanamitsu, M., Kistler, R., Collins, W., Deaven, D., Gandin, L., Iredell, M., Saha, S., White, G., Woollen, J., Zhu, Y., Leetmaa, A., Reynolds, R., Chelliah, M., Ebisuzaki, W., Higgins, W., Janowiak, J., K. C. Mo, Ropelewsky, C., Wang, J., Jennec, R., and Joseph, D.: The NCEP/NCAR 40-Year Reanalysis Project, Bullet. Am. Meteorol. Soc., 77, 437–471, 1996.

Laanbroek, H. J.: Methane emission from natural wetlands: interplay between emergent macrophytes and soil microbial processes. A mini-review, Ann. Botany, 105, 141–153, doi:10.1093/aob/mcp201, 2010.

Lemoine, J.-M., Bruinsma, S., Loyer, S., Biancale, R., Marty, J.-C., Perosanz, F., and Balmino, G.: Temporal gravity field models inferred from GRACE data, Adv. Space Res., 39, 1620–1629, doi:10.1016/j.asr.2007.03.062, 2007.

Lewis, S. L., Brando, P. M., Phillips, O. L., van der Heijden, G. M. F., and Nepstad, D.: The 2010 Amazon Drought, Science, 331, 554, doi:10.1126/science.1200807, 2011.

Longhi, D., Bartoli, M., and Viaroli, P.: Decomposition of four macrophytes in wetland sediments: Organic matter and nutri-

ent decay and associated benthic processes, Aquatic Botany, 89, 303–310, doi:10.1016/j.aquabot.2008.03.004, 2008.

Malhi, Y., Aragao, L. E. O. C., Metcalfe, D. B., Paiva, R., Quesada, C. A., Almeida, S., Anderson, L., Brando, P., Chambers, J. Q., Da Costa, A. C. L., Hutyra, L. R., Oliveira, P., Patino, S., Pyle, E. H., Robertson, A. L., and Teixeira, L. M.: Comprehensive assessment of carbon productivity, allocation and storage in three Amazonian forests, Global Change Biol., 15, 1255–1274, doi:10.1111/j.1365-2486.2008.01780.x, 2009.

Melack, J. M., Hess, L. L., Gastil, M., Forsberg, B. R., Hamilton, S. K., Lima, I. B. T., and Nova, E. M. L. M.: Regionalization of methane emissions in the Amazon basin with microwave remote sensing, Global Change Biol., 10, 530–544, 2004.

Mitsch, W., Nahlik, A., Wolski, P., Bernal, B., Zhang, L., and Ramberg, L.: Tropical wetlands: seasonal hydrologic pulsing, carbon sequestration, and methane emissions, Wetlands Ecol. Manage., 18, 573–586, doi:10.1007/s11273-009-9164-4, 2010.

Miyajima, T., Wada, E., Hanba, Y. T., and Vijarnsorn, P.: Anaerobic mineralization of indigenous organic matters and methanogenesis in tropical wetland soils, Geochimica et Cosmochimica Acta, 61, 3739–3751, doi:10.1016/S0016-7037(97)00189-0, 1997.

Neue, H., Wassmann, R., Kludze, H., Bujun, W., and Lantin, R.: Factors and processes controlling methane emissions from rice fields, Nutr. Cycl. Agroecosys., 49, 111–117, 1997.

Oki, T. and Sud, Y. C.: Design of Total Runoff Integrating Pathways (TRIP) – A global river channel network, Earth Interactions, 2, 1–37, 1998.

Papa, F., Güntner, A., Frappart, F., Prigent, C., and Rossow, W. B.: Variations of surface water extent and water storage in large river basins: A comparison of different global data sources, Geophys. Res. Lett., 351, L11401, doi:10.1029/2008GL033857, 2008.

Pierobon, E., Bolpagni, R., Bartoli, M., and Viaroli, P.: Net primary production and seasonal CO$_2$ and CH$_4$ fluxes in a Trapa natans L. meadow, J. Limnol., 69, 2010.

Prigent, C., Papa, F., Aires, F., Rossow, W. B., and Matthews, E.: Global inundation dynamics inferred from multiple satellite observations, 1993–2000, J. Geophys. Res. Atmos., 112, D12107, doi:10.1029/2006JD007847, 2007.

Prinn, R. G., Weiss, R. F., Fraser, P. J., Simmons, P. G., Cunnold, D. N., Alyea, F. N., O'Doherty, S., Salameh, P., Miller, B. R., Huang, J., Wang, R. H. J., Hartley, D. E., Harth, C., Steele, L. P., Sturrock, G., Midgley, P. M., and McCulloch, A.: A History of Chemically and Radiatively Important Gases in Air deduced from ALE/GAGE/AGAGE, J. Geophys. Res., 105, 17751–17792, 2000.

Riley, W. J., Subin, Z. M., Lawrence, D. M., Swenson, S. C., Torn, M. S., Meng, L., Mahowald, N. M., and Hess, P.: Barriers to predicting changes in global terrestrial methane fluxes: analyses using CLM4Me, a methane biogeochemistry model integrated in CESM, Biogeosciences, 8, 1925–1953, doi:10.5194/bg-8-1925-2011, 2011.

Ringeval, B., de Noblet-Ducoudré, N., Ciais, P., Bousquet, P., Prigent, C., Papa, F., and Rossow, W. B.: An attempt to quantify the impact of changes in wetland extent on methane emissions on the seasonal and interannual time scales, Global Biogeochem. Cyc., 24, GB2003, doi:10.1029/2008GB003354, 2010.

Schmidt, H., Eickhorst, T., and Tippkötter, R.: Monitoring of root growth and redox conditions in paddy soil rhizotrons by redox electrodes and image analysis, Plant Soil, 341, 221–232,

http://dx.doi.org/10.1007/s11104-010-0637-2, 10.1007/s11104-010-0637-2, 2011.

Schubert, C., Lucas, F., Durisch-Kaiser, E., Stierli, R., Diem, T., Scheidegger, O., Vazquez, F., and Müller, B.: Oxidation and emission of methane in a monomictic lake (Rotsee, Switzerland), Aquatic Sciences – Research Across Boundaries, 72, 455–466, doi:10.1007/s00027-010-0148-5, 2010.

Seybold, C., Mersie, W., Huang, J., and McNamee, C.: Soil redox, pH, temperature, and water-table patterns of a freshwater tidal wetland, Wetlands, 22, 149–158, doi:10.1672/0277-5212(2002)022[0149:SRPTAW]2.0.CO;2, 2002.

Silva, T., Costa, M., and Melack, J.: Annual net primary production of macrophytes in the eastern Amazon floodplain, Wetlands, 29, 747–758, doi:10.1672/08-107.1, 2009.

Singh, S.: Exploring correlation between redox potential and other edaphic factors in field and laboratory conditions in relation to methane efflux, Environ. Int., 27, 265–274, doi:10.1016/S0160-4120(01)00055-1, 2001.

Singh, S., Kulshreshtha, K., and Agnihotri, S.: Seasonal dynamics of methane emission from wetlands, Chemosphere - Global Change Science, 2, 39–46, doi:10.1016/S1465-9972(99)00046-X, 2000.

Sitch, S., Smith, B., Prentice, I. C., Arneth, A., Bondeau, A., Cramer, W., Kaplan, J. O., Levis, S., Lucht, W., Sykes, M. T., Thonicke, K., and Venevsky, S.: Evaluation of ecosystem dynamics, plant geography and terrestrial carbon cycling in the LPJ dynamic global vegetation model, Global Change Biol., 9, 161–185, doi:10.1046/j.1365-2486.2003.00569.x, 2003.

Tapley, B. D., Bettadpur, S., Ries, J. C., Thompson, P. F., and Watkins, M. M.: GRACE Measurements of Mass Variability in the Earth System, Science, 305, 503–506, doi:10.1126/science.1099192, 2004.

Thompson, Y., Sandefur, Brian abd Karathanasis, A., and D'angelo, E.: Redox Potential and Seasonal Porewater Biogeochemistry of Three Mountain Wetlands in Southeastern Kentucky, USA, Aquat. Geochem., 15, 349–370, doi:10.1007/s10498-008-9042-3, 2009.

Wahr, J., Swenson, S., Zlotnicki, V., and Velicogna, I.: Time-variable gravity from GRACE: First results, Geophys. Res. Lett., 31, 11501, doi:10.1029/2004GL019779, 2004.

Walter, B. P., Heimann, M., and Matthews, E.: Modelling modern methane emissions form natural wetlands 1. Model description and results, J. Geophys. Res., 106, 34189–34206, 2001.

Wania, R., Ross, I., and Prentice, I. C.: Implementation and evaluation of a new methane model within a dynamic global vegetation model: LPJ-WHyMe v1.3.1, Geosci. Model Dev., 3, 565–584, doi:10.5194/gmd-3-565-2010, 2010.

Whalen, S. C.: Biogeochemistry of Methane Exchange between Natural Wetlands and the Atmosphere, Environ. Eng. Sci., 22, 73–95, 2005.